



**HAL**  
open science

## Water transfer in soil at low water content. Is the local equilibrium assumption still appropriate?

Francois Ouedraogo, Fabien Cherblanc, Bétaboalé Naon, Jean-Claude Benet

► **To cite this version:**

Francois Ouedraogo, Fabien Cherblanc, Bétaboalé Naon, Jean-Claude Benet. Water transfer in soil at low water content. Is the local equilibrium assumption still appropriate?. *Journal of Hydrology*, 2013, 492, pp.117-124. 10.1016/j.jhydrol.2013.04.004 . hal-00809260

**HAL Id: hal-00809260**

**<https://hal.science/hal-00809260>**

Submitted on 8 Apr 2013

**HAL** is a multi-disciplinary open access archive for the deposit and dissemination of scientific research documents, whether they are published or not. The documents may come from teaching and research institutions in France or abroad, or from public or private research centers.

L'archive ouverte pluridisciplinaire **HAL**, est destinée au dépôt et à la diffusion de documents scientifiques de niveau recherche, publiés ou non, émanant des établissements d'enseignement et de recherche français ou étrangers, des laboratoires publics ou privés.

# Water transfer in soil at low water content. Is the local equilibrium assumption still appropriate?

F. Ouedraogo<sup>a</sup>, F. Cherblanc<sup>b,\*</sup>, B. Naon<sup>a</sup>, J.-C. Béné<sup>b</sup>

<sup>a</sup>*GERME & TI, Université Polytechnique de Bobo Dioulasso, Burkina Faso*

<sup>b</sup>*LMGC, CNRS, Université Montpellier 2, Place Eugène Bataillon  
34000 Montpellier, France*

---

## Abstract

The dynamics of water content in the superficial layers of soils is critical in the modelling of land-surface processes. In arid regions, vapour flux contributes significantly to the global water mass balance. To account for it in theoretical descriptions, most of the models proposed in the literature rely on the local equilibrium assumption that constrains the vapour pressure to remain at its equilibrium value. It implicitly amounts to consider an instantaneous phase change. Recent works underlined a retardation time and a decrease in phase change rate as the water content gets lower. Therefore, the objective is to revisit water transport modelling by rejecting the local equilibrium assumption. This requires developing a non-equilibrium model by taking into account the phase change kinetics. To assess the interest of this approach, a natural soil of Burkina-Faso has been experimentally characterized from independent tests and soil column experiments have been carried out. The comparison of experimental drying kinetics and water content pro-

---

\*Corresponding author – E-mail: fabien.cherblanc@univ-montp2.fr – Tel: (+33) 467-149-639 – Fax: (+33) 467-144-555

files with computational predictions confirms the reliability of this description. Liquid/gas non-equilibrium is significant in a limited subsurface zone which defines explicitly the transition from liquid transport in lower layers to vapour transport in upper layers, i.e., the evaporation front. The overall moisture dynamics is governed by the coupling between water transport mechanisms (liquid filtration, vapour diffusion, phase change) that mainly occurs in this transition zone.

*Keywords:* water transport, evaporation, non-equilibrium, experimental, modelling

---

## 1. Introduction

Land–atmosphere mass exchanges are concentrated in the superficial layers of soils and control most of biological processes required for plant growth. An accurate description of these layers is of first importance when developing realistic boundary conditions to be implemented in large-scale environmental models. Intensive research has been done to develop efficient numerical models of water transport in the vadose zone. In particular, the quantification of total water evaporation from soil is a crucial issue since it governs the water content dynamics near the surface (Gowing et al., 2006).

Following the pioneered work of Philip and de Vries (1957), most of models have associated the Richard’s equation in the liquid phase with a classical diffusive equation in the gas phase while both transport phenomena are coupled through the heat equation (Bittelli et al., 2008; Garcia-Gonzalez et al., 2012; Grifoll et al., 2005; Novak, 2010; Parlange et al., 1998; Saito et al., 2006; Sakai et al., 1999; Thomas and Missoum, 1999; Xiang et al., 2012;

16 Yanful and Mousavi, 2003). Although thermal gradients affect liquid water  
17 redistribution in soils, the most important coupling process is the transport  
18 of latent heat by vapour flux. These models have been successfully used to  
19 describe the land-atmosphere water and energy balance of various natural  
20 field soils over a large period (Bittelli et al., 2008; Garcia-Gonzalez et al.,  
21 2012; Grifoll et al., 2005; Novak, 2010; Saito et al., 2006).

22 Most of these models have been developed for temperate regions where  
23 water content evolves in the capillary domain from saturation to the melting  
24 point. Since water vapour flow in semi-arid and arid regions can represent a  
25 major part of the overall water flow, it is important to take it into account  
26 together with liquid water flow when evaluating hydrologic fluxes (Garcia-  
27 Gonzalez et al., 2012; Sakai et al., 1999). In this framework, classical models  
28 have been extrapolated towards low water contents without carefully check-  
29 ing the validity of such formulations. For instance, usual descriptions of the  
30 water retention curve can significantly diverge from experimental points at  
31 very low water content (Thakur et al., 2006). Correction functions have been  
32 proposed without being fully satisfactory. However, as water content goes  
33 to very low values, liquid water takes the form of adsorbed layers onto solid  
34 surface and does not behave as “free” water. It has been shown that film  
35 flows replace conventional capillary flows at low water content, induces a  
36 change in the relative permeability description (Tuller and Or, 2002). It is  
37 therefore noteworthy to consider that modelling water transport phenomena  
38 at low water content calls for a specific description.

39 In particular, the *local equilibrium assumption* is extensively used in most  
40 of the theoretical models proposed in the literature (Bittelli et al., 2008;

41 Garcia-Gonzalez et al., 2012; Grifoll et al., 2005; Novak, 2010; Parlange et al.,  
42 1998; Saito et al., 2006; Sakai et al., 1999; Thomas and Missoum, 1999; Xi-  
43 ang et al., 2012; Yamanaka and Yonetani, 1999; Yanful and Mousavi, 2003).  
44 This hypothesis governs the liquid/gas mass exchange by assuming that the  
45 partial pressure of vapour remains equal to its equilibrium value. It is gen-  
46 erally written as an explicit relation between the relative humidity and the  
47 hydraulic head. It allows combining liquid and vapour mass balance equa-  
48 tions in a single one describing the global soil moisture content. Implicitly, it  
49 amounts to consider that the evaporation process is instantaneous in compar-  
50 ison with the other transport phenomena. This should be fairly satisfactory  
51 when capillary forces are predominant. Nevertheless, under particular condi-  
52 tions, a volatilization retardation time has been observed (Armstrong et al.,  
53 1994; Bénet and Jouanna, 1982; Chammari et al., 2008). In the hygroscopic  
54 domain where adsorption phenomena predominate, phase change kinetics is  
55 strongly influenced by the thermodynamic state of water and evaporation  
56 rate is drastically reduced (Bénet et al., 2009; Lozano et al., 2008). These  
57 experimental observations conducted us to reconsider the *local equilibrium*  
58 *assumption* in order to assess its reliability.

59 The aim of this contribution is to revisit water transport modelling in the  
60 lower range of water content. The prominence of hygroscopic effects leads  
61 us to reject the liquid/gas equilibrium assumption. This requires developing  
62 a two-equation model by taking into account the phase change kinetics. It  
63 means that, in some specific configurations, the characteristic times of the  
64 three transport mechanisms considered (liquid flow, vapour diffusion, liquid-  
65 gas phase change) are of the same order of magnitude. To fulfil this objective,

66 a natural soil of Burkina-Faso has been experimentally characterized from  
67 independent tests and soil column experiments have been carried out. The  
68 comparison of experimental drying kinetics and water content profiles with  
69 computational predictions supports the validation of this description. There-  
70 fore, the *local equilibrium assumption* can be discussed based on numerical  
71 simulations. In particular, the location of the evaporation front is identified  
72 as it propagates from the upper surface towards deeper layers.

## 73 **2. Theoretical and numerical modelling of water transfer**

### 74 *2.1. Liquid and vapour transfer model*

75 A natural soil can be idealized by a triphasic porous medium by consid-  
76 ering a solid, a liquid and a gaseous phase, while the gaseous phase consists  
77 of two components: dry air and water vapour. Theoretical modelling relies  
78 on the following assumptions:

- 79 • Temperature is uniform and constant. This hypothesis will be validated  
80 *a posteriori* in the last section based on numerical simulations.
- 81 • The solid skeleton is undeformable. Assuming a rigid structure is a  
82 strong hypothesis since evaporation and dehydration processes in non-  
83 consolidated soils generally lead to global shrinkage. However, we focus  
84 our attention on the hygroscopic domain where these effects are negli-  
85 gible.
- 86 • The total gas pressure is constant and uniform, since the convective  
87 transport in the gas phase is negligible. Actually, it means that the gas  
88 permeability is large enough to assume that a pressure gradient will

89 be instantaneously equilibrated when compared to the other transport  
 90 phenomena.

Therefore, three elementary phenomena are considered: liquid filtration governed by capillary and gravity effects, vapour diffusion in the gas phase and liquid-gas phase change of water. Fundamental mass balance equations of water in liquid and gas phase are written:

$$\frac{\partial \rho_l}{\partial t} + \nabla \cdot (\rho_l \mathbf{v}_l) = -\hat{\rho}_v \quad (1)$$

$$\frac{\partial \rho_v}{\partial t} + \nabla \cdot \mathbf{J}_v = \hat{\rho}_v \quad (2)$$

91 where  $\rho_l$  and  $\rho_v$  ( $\text{kg m}^{-3}$ ) are, respectively, the apparent density of liquid  
 92 water and its vapour,  $\mathbf{v}_l$  ( $\text{m s}^{-1}$ ) is the intrinsic velocity of liquid water  
 93 and  $\mathbf{J}_v$  ( $\text{kg m}^{-2} \text{s}^{-1}$ ) is the vapour diffusion flux. The phase-change rate  $\hat{\rho}_v$   
 94 ( $\text{kg m}^{-3} \text{s}^{-1}$ ) is thus a volumetric scalar flux, representing the mass of water  
 95 transforming from a liquid state to a vapour state by unit volume and unit  
 96 time.

97 From an experimental point of view, appropriate state variables are the  
 98 mass water content,  $w(\%)$ , defined as the ratio between the apparent mass  
 99 densities of liquid and solid:

$$w = \frac{\rho_l}{\rho_s} \quad (3)$$

100 and the vapour partial pressure in the gas phase,  $p_v(\text{Pa})$ , linked to the ap-  
 101 parent density of vapour,  $\rho_v$ , through the ideal gas law:

$$\phi_g p_v = \frac{RT}{M_w} \rho_v \quad (4)$$

102 where  $R$  ( $\text{J kg}^{-1}$ ) is the ideal gas constant and  $M_w$  ( $\text{kg}$ ) is the molar mass  
 103 of water. The volume fraction of the gas phase,  $\phi_g$ , is related to the water

104 content by:

$$\phi_g = \frac{V_g}{V} = 1 - \frac{\rho_s}{\rho_s^*} - w \frac{\rho_s}{\rho_l^*} \quad (5)$$

105 where  $\rho_s^*$  and  $\rho_l^*$  ( $\text{kg m}^{-3}$ ) are, respectively, the real density of solid and liquid  
106 phase.

### 107 2.2. Vapour diffusion

108 The vapour diffusion flux,  $\mathbf{J}_v$ , is classically described by a first order Fick's  
109 law:

$$\mathbf{J}_v = -D_{vs} \nabla \rho_v^* \quad (6)$$

110 where  $D_{vs}$  is the effective vapour diffusion coefficient in the soil. It gen-  
111 erally depends on the tortuosity as presented in next section dealing with  
112 experimental characterization.

### 113 2.3. Liquid filtration

114 The liquid filtration flux appearing in Eq. 1 can be expressed by the  
115 Darcy's law extended to the non-saturated case. The validity of such de-  
116 scription toward very low water content is questionable since the concept of  
117 liquid pressure is meaningless (Baker and Frydman, 2009; Low, 1961; Nitao  
118 and Bear, 1996). An alternative proposed by Bénet et al. (2012) is to rely  
119 on the chemical potential. Therefore, filtration transport is written:

$$\rho_l \mathbf{v}_l = -K (\nabla \mu_l - \mathbf{g}) \quad (7)$$

120 where  $\mu_l$  ( $\text{J kg}^{-1}$ ) is the mass chemical potential of liquid water,  $\mathbf{g}$  ( $\text{m s}^{-2}$ ) is  
121 the gravity acceleration vector. The filtration coefficient,  $K$ , refers to the soil  
122 effective conductivity by means of:

$$K = K_r K_{sat} \frac{\rho_l^*}{g} \quad (8)$$

123 where  $K_r$  is the relative permeability function and  $K_{sat}$  ( $\text{m s}^{-1}$ ) the hydraulic  
124 conductivity at saturation.

125 The chemical potential is a function of the water content described by  
126 the soil/water retention curve. It is usually built by merging measurements  
127 from classical tensiometry and sorption isotherm. Depending on the research  
128 area (civil, petrol or food engineering, agronomy, pedology), various names  
129 are used to designate this potential (suction, soil matrix potential, capillary  
130 pressure, liquid activity). The chemical potential can be seen as a unifying  
131 concept well defined in a thermodynamic framework (Job and Hermann,  
132 2006). From its energetic definition, the chemical potential can consistently  
133 describe the thermodynamic state of water over the whole range of water  
134 content (Bénet et al., 2012).

#### 135 *2.4. Liquid-gas phase change*

136 From thermodynamic considerations, it can be shown that the volumetric  
137 rate of phase change  $\hat{\rho}$  ( $\text{kg m}^{-3} \text{ s}^{-1}$ ) is proportional to the water chemical  
138 potential difference between the liquid and vapour states (Bedeaux and Kjel-  
139 strup, 2004; Bénet and Jouanna, 1982; Kuiken, 1994). A detailed develop-  
140 ment of this phase change theoretical relation has been given by Bénet et al.  
141 (2009) and the main results are recalled here. In the isothermal case, the  
142 non-equilibrium phase change rate is expressed as a function of the vapour  
143 partial pressure by:

$$\hat{\rho}_v = -L \frac{R}{M_w} \ln \left( \frac{p_v}{p_{veq}} \right) \quad (9)$$

144 where  $L$  ( $\text{kg K s m}^{-5}$ ) is a phenomenological coefficient to be determined ex-  
145 perimentally as detailed in next section. The vapour pressure at equilibrium,

146  $p_{veq}$ , is defined as the product of the saturating vapour pressure at the given  
 147 temperature multiplied by the water activity:

$$p_{veq} = a_w(w) p_{vs}(T) \quad (10)$$

148 The liquid activity is defined by the sorption isotherm curve. Since it is  
 149 an equilibrium properties, it can only describe an equilibrium situation as  
 150 required by the local equilibrium assumption. Rejecting this fundamental  
 151 hypothesis means that the vapour pressure,  $p_v$ , can diverge from its equilib-  
 152 rium value,  $p_{veq}$ .

### 153 2.5. Numerical discretization

154 Finally, mass balance equations are written:

$$\frac{\partial w}{\partial t} - K_{sat} \frac{\rho_e^*}{\rho_s g} \nabla \cdot \left( K_r \frac{\partial \mu_l}{\partial w} \nabla w - K_r \mathbf{g} \right) - L \frac{R}{\rho_s M_w} \ln \left( \frac{p_v}{p_{veq}} \right) = 0 \quad (11)$$

$$\frac{\partial}{\partial t} (\phi_g p_v) - \nabla \cdot (D_{vs} \nabla p_v) + L \frac{R^2 T}{M_w^2} \ln \left( \frac{p_v}{p_{veq}} \right) = 0 \quad (12)$$

156 These non-linear equations are strongly coupled, on one hand, through the  
 157 phase change term,  $\hat{\rho}_v$ , and on the other hand, through physical characteris-  
 158 tics that depends on the water content:  $\phi_g(w)$ ,  $D_{vs}(w)$ ,  $L(w)$ .

159 Balance equations are discretized based on finite-volume formulation us-  
 160 ing a one-dimensional regular mesh where the unknowns,  $w$  and  $p_v$  are located  
 161 at the centre of grid blocks. A first-order upstream scheme is used to describe  
 162 the convective term appearing in the liquid mass balance. Temporal integra-  
 163 tion is performed using a fully implicit scheme to get numerical stability. To  
 164 handle with non-linearities, a Newton-Raphson method ensures an accurate  
 165 convergence for a moderate time step.

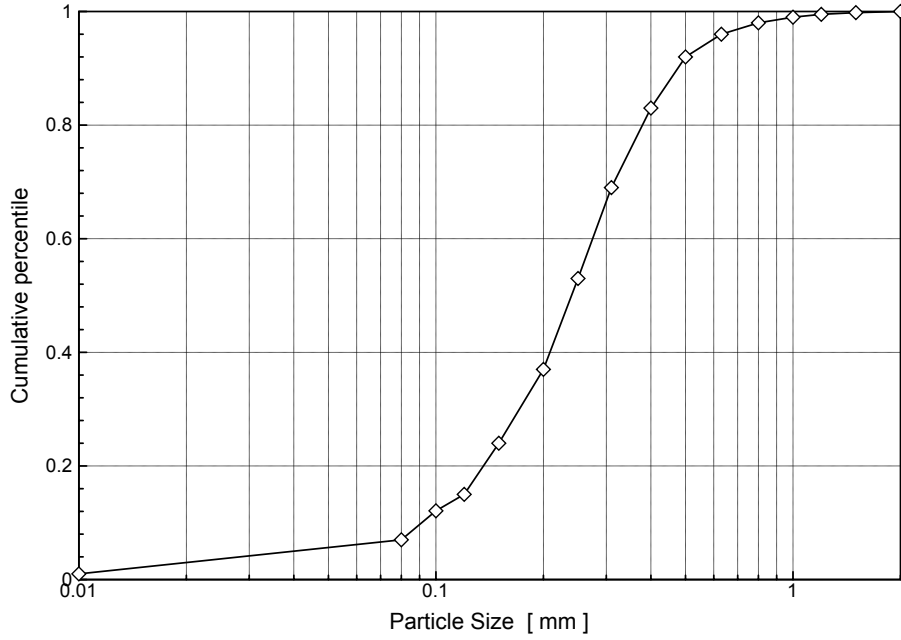


Figure 1: Soil granulometric curve.

166 **3. Materials: a typical soil from Burkina-Faso**

167 The material under investigation is a natural soil from Nasso, Burkina-  
 168 Faso. From its particle size distribution (Fig. 1), this soil can be classified as  
 169 a fine sand, the silty or clayey fraction is almost negligible. This is in agree-  
 170 ment with the sorption isotherm curve which highlights a limited hygroscopic  
 171 domain that ranges from 0% to 2% (Fig. 2).

172 *3.1. Vapour diffusion*

173 Through Fick's equation (Eq. 6), the vapour diffusion flux depends on  
 174 the effective diffusion coefficient in soil,  $D_{vs}$ . It is generally defined as:

$$D_{vs} = \tau \phi_g D_{va} \tag{13}$$

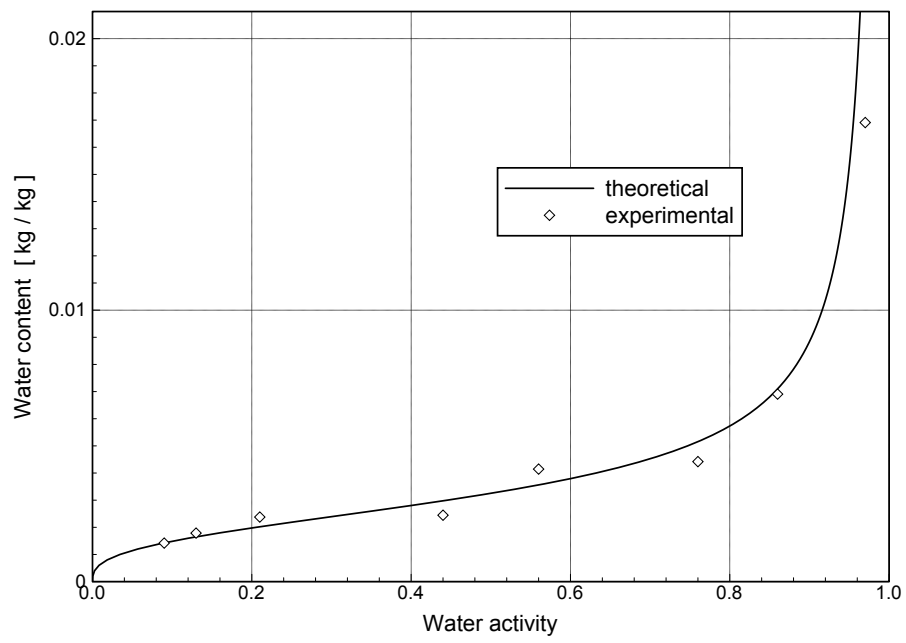


Figure 2: Experimental sorption isotherm curve and theoretical modelling (Fredlund et al., 2002).

175 where  $\tau$  represents the tortuosity and  $D_{va}$  the free diffusion coefficient of  
176 vapour in air. Standard correlation gives a value at 30°C,  $D_{va} = 26.1 \times$   
177  $10^{-6} \text{ m s}^{-2}$  (Campbell, 1985). Several relations have been proposed to de-  
178 scribe the tortuosity coefficient as a function soil characteristics (Abu-El-Shar  
179 and Abriola, 1997; Moldrup et al., 2000). The classical relation proposed by  
180 Millington & Quirck (Moldrup et al., 2001) has been chosen:

$$\tau = \phi_g^{\frac{7}{3}} / \phi^2 \quad (14)$$

181 Anyway, numerical simulations have brought out a weak dependence of total  
182 water transport on the diffusion model. Regarding the case under investiga-  
183 tion, the various relations proposed in the literature are roughly equivalent.

### 184 3.2. *Liquid filtration*

185 The soil water retention curve has been determined by merging measures  
186 from tensiometry and sorption isotherm. This is based on classical devices  
187 such as the pressure plate and standard saline solutions. Relying on both ex-  
188 perimental techniques leads to characterize the soil/water equilibrium state  
189 over the whole range of water content. As discussed by Bénet et al. (2012),  
190 a variety of micro-scale mechanisms governs the soil/water interaction. De-  
191 scribing their macro-scale manifestation by means of pressure head or suction  
192 is meaningless in the low water content range. The classical theory based on  
193 capillary effects leads to misinterpretations and cannot be extended without  
194 careful investigation. Therefore, the chemical potential is more appropri-  
195 ate. Following this point of view, the soil/water retention curve (Fig. 3) is  
196 presented with the water mass chemical potential in abscissa.

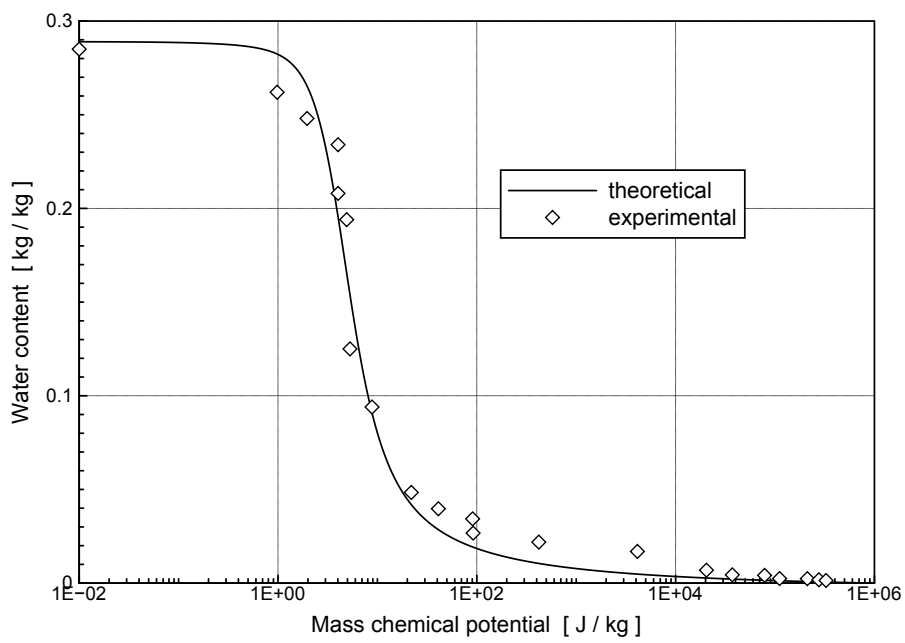


Figure 3: Experimental and fitted theoretical soil water retention curve (Fredlund and Xing, 1994).

197 Several models have been presented in the literature to represent the  
 198 soil/water retention curve. By analysing the behaviour of several soils,  
 199 Thakur et al. (2006) highlighted that the fitting function proposed by Fred-  
 200 lund and Xing (1994) is the most appropriate description valid for very low  
 201 water content. This model is given by:

$$w = \left[ 1 - \frac{\ln \left( 1 + \frac{\mu}{\mu_r} \right)}{\ln \left( 1 + \frac{10^6}{\mu_r} \right)} \right] \frac{w_{sat}}{\left[ \ln \left( e + \left( \frac{\mu}{\mu_i} \right)^n \right) \right]^m} \quad (15)$$

202 where  $\mu_r$ ,  $\alpha$ ,  $n$  and  $m$  are soil parameters. Numerical identification with  
 203 experimental points lead to values:  $\mu_i = 3.78$ ,  $\mu_r = 9.02$ ,  $n = 2.87$  and  
 204  $m = 1.10$ , as represented in Fig. 3.

205 The hydraulic conductivity at saturation,  $K_{sat}$ , was measured experi-  
 206 mentally with saturated samples compacted to reach a solid apparent mass  
 207 density,  $\rho_s = 1500 \text{ kg m}^3$ , which corresponds to a porosity,  $\phi = 43\%$ . The  
 208 average value obtained from several trials is:  $K_{sat} = 3.995 \times 10^{-6} \text{ m s}^{-1}$ .

209 The relative permeability function,  $K_r$ , is assumed to be described by the  
 210 Mualem's predictive model explicated in the case of the soil/water retention  
 211 curve proposed by Van Genuchten (1980). The mathematical development  
 212 leads to the following relation (Van Genuchten and Nielsen, 1985):

$$K_r = \sqrt{S_e} \left[ 1 - \left( 1 - S_e^{\frac{1}{m}} \right)^m \right]^2 \quad (16)$$

213 where the effective saturation,  $S_e$ , is defined by

$$S_e = \frac{w - w_{res}}{w_{sat} - w_{res}} \quad (17)$$

214 The water content at saturation,  $w_{sat}$ , the residual water content,  $w_{res}$ , and  
 215 the exponent,  $m$ , are soils characteristic identified on the soil water reten-  
 216 tion curve (Fig. 3) using the relation proposed by Van Genuchten (1980).

217 Parameter values obtained from the numerical identification procedure are:  
218  $w_{sat} = 0.289$ ,  $w_{res} = 0.00942$ ,  $m = 0.526$ .

### 219 *3.3. Liquid-gas phase change*

220 The phase change coefficient,  $L$ , introduced in this relation, should de-  
221 pends on the state variables such as the water content, the temperature and  
222 on the nature of the soil. This coefficient must be determined experimentally  
223 and has been the focus of several works (Lozano et al., 2008, 2009; Ruiz and  
224 Bénét, 2001). An original experimental device has been developed to analyse  
225 the return back to equilibrium of a soil sample subjected to non-equilibrium  
226 conditions. This non-equilibrium situation is caused by, first, extracting the  
227 gas phase of the soil sample, and then, replacing it by dry air, what results  
228 in a macroscopic thermodynamic non-equilibrium between the liquid phase  
229 and its vapour. Thus, the dependence of the phase change coefficient  $L$  on  
230 several physical variables (temperature, water content, total gas pressure)  
231 has been experimentally investigated (Lozano et al., 2009; Ruiz and Bénét,  
232 2001). The influences of the nature of the liquid and of the soil texture have  
233 also been underlined.

234 From a large set of experimental data carried out in isothermal conditions  
235 with pure water in clayey silty sand, Lozano et al. (2008) have provided a  
236 complete model of the phase change coefficient. Its variations as functions  
237 of the water content and the vapour partial pressure are characterised by 3  
238 coefficients ( $L_{eq}$ ,  $k$ ,  $r$ ) through the following expressions:

$$\text{close to equilibrium, i.e., } r \leq \frac{p_v}{p_{veq}} \leq 1 \quad : \quad L = L_{eq} \quad (18)$$

239

far from equilibrium, i.e.,  $0 \leq \frac{p_v}{p_{veq}} \leq r$  :  $L = L_{eq} + k \left( r - \frac{p_v}{p_{veq}} \right)$  (19)

240 The neighbourhood of an equilibrium situation, i.e., when the vapour partial  
 241 pressure is close to its equilibrium value, corresponds to the validity domain  
 242 of the linear thermodynamics of irreversible processes and a constant phe-  
 243 nomenological coefficient is observed. Outside of this domain, i.e., far from  
 244 equilibrium, an affine dependence on the vapour partial pressure is obtained  
 245 and the phase change rate is highly increased. Concerning the soil under  
 246 investigation, the influence of the water content on model parameters ( $L_{eq}$ ,  
 247  $r$ ) is presented in Figs. 4 and 5 while the third parameter  $r$  has be found  
 248 to be fairly constant,  $r = 0.93$ . Some bell-shaped curves are generally ob-  
 249 served, where the maximum around 3% is roughly the upper limit of the  
 250 hygroscopic domain. Above this maximum, the phase change rate decreases  
 251 since the liquid-gas interface area reduces. For water content greater than  
 252 7%, the gas phase is occluded and phase change cannot be activated. Below  
 253 the maximum, when hygroscopic effects become predominant, the intensity  
 254 of solid-liquid interactions increases in the adsorbed layers. The supplemen-  
 255 tary energy required for water desorption decreases the phase change rate  
 256 leading to lower values of the coefficient.

## 257 4. Validation: laboratory column experiments

### 258 4.1. Laboratory column experiments

259 Homogenized wet soil was compacted in a PVC tube to reach a solid  
 260 apparent mass density,  $\rho_s = 1500 \text{ kg m}^3$ , which corresponds to a porosity,  $\phi =$

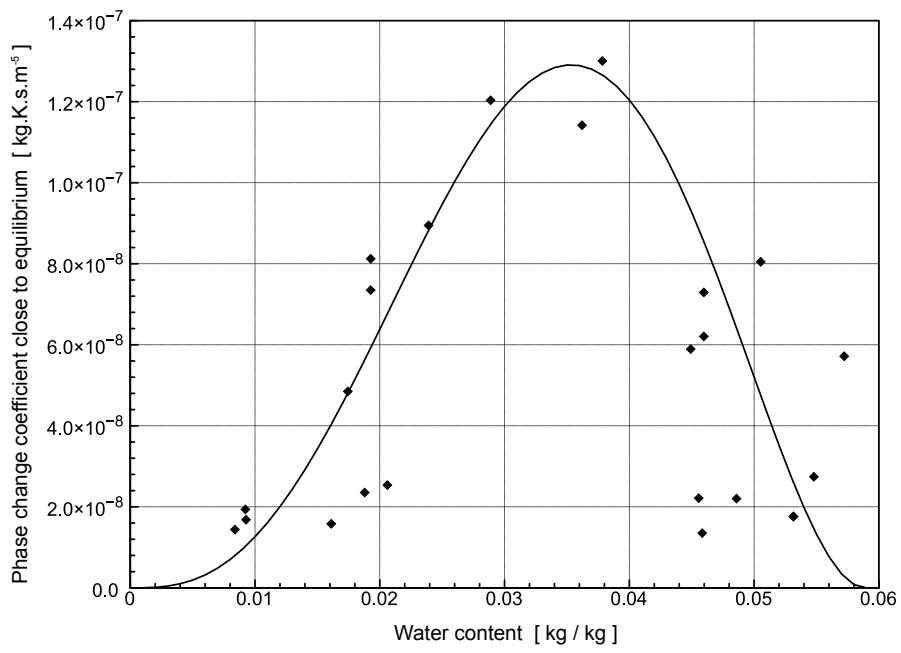


Figure 4: Phenomenological coefficient close to equilibrium,  $Leq$ , versus the water content,  $w$ . Experimental points and fitting relation.

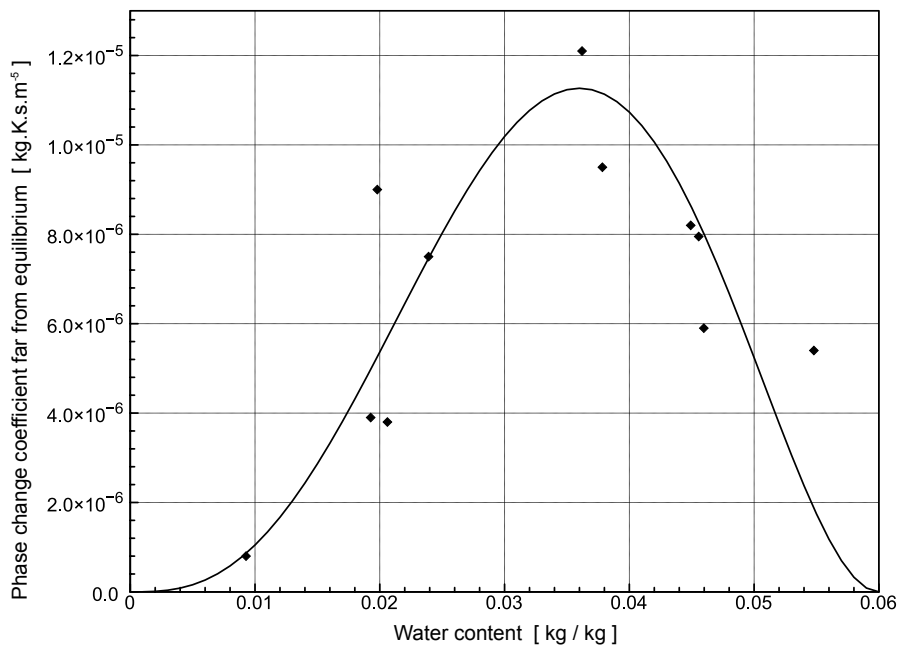


Figure 5: Phenomenological coefficient far from equilibrium,  $k$ , versus the water content,  $w$ . Experimental points and fitting relation.

261 43%. Sample dimensions were 30 cm height and 7.5 cm diameter. The initial  
262 water content of the soil was fixed at  $w = 6\%$  to focus on low water content  
263 cases. Then, soil samples were placed in a regulated drying atmosphere at  
264 controlled temperature  $T = 30^\circ\text{C}$  and relative humidity  $RH_1 = 30\%$  for  
265 the first case, and  $RH_2 = 50\%$  for the second case. The lower surface was  
266 hermetically closed while the upper surface was in contact with air.

267 Columns were weighed at regular time steps to determine the average  
268 water content leading to the drying kinetics plotted in Figs. 6 and 7. In  
269 each case ( $RH_1 = 30\%$  and  $RH_2 = 50\%$ ), the six experimental kinetics were  
270 achieved with a good reproducibility. The determination of water content  
271 profiles was based on a destructive method. Indeed, soil columns were cut  
272 into 2 cm slices and water content was measured by differential weighing  
273 after 48 hours drying at  $105^\circ\text{C}$ .

274 The evolutions of water content profiles presented in Figs. 8 and 9 clearly  
275 highlight water transport towards the upper side. Surface water content  
276 quickly decreases to the residual water content given by the soil/water reten-  
277 tion curve (Fig. 3):  $w_{res} \approx 0.01$ . At beginning, one can observe that the water  
278 content at bottom slightly exceeds the initial water content. This underlines  
279 that, in this range of water content, gravitational and capillary forces are of  
280 the same order of magnitude.

#### 281 *4.2. Comparison with theoretical model*

282 Using identical boundary and initial conditions, numerical simulation of  
283 Eqs. 11 and 12 are plotted in solid line on Figs. 6 through 9. A very good  
284 agreement between the experimental drying kinetics and theoretical predic-  
285 tions is obtained in both cases (Figs. 6 and 7). Furthermore, numerical sim-

286 ulations are able to fairly represent the overall evolutions of water content  
287 profiles (Figs. 8 and 9).

288 Even if the overall agreement is good, some local discrepancies are ob-  
289 served. For instance, at the end of experiments, the gradient of water con-  
290 tent is roughly constant what numerical profiles cannot represent. This is-  
291 sue mainly depends on the relative permeability description (Eq. 16) which  
292 has not been developed specifically for the soil under investigation. Further  
293 experimental characterization is required to completely define the specific  
294 relative permeability relation associated with this soil. Anyway, by relying  
295 on the literature, the relation chosen in this case seems to be appropriate.

296 On can notice an evaporation front that penetrates inside the soil column  
297 from the top (Rose et al., 2005; Yamanaka and Yonetani, 1999). It corre-  
298 sponds to the propagation of the upper boundary condition through the soil  
299 resulting from diffusion and phase change processes. Therefore, a major issue  
300 is that the response of soil columns to the imposed relative humidity is ade-  
301 quately represented by our numerical model. Without any fitting parameter,  
302 the competition of three phenomena (filtration, diffusion and phase change)  
303 is an accurate description of water transport in soils.

## 304 **5. Is liquid/gas equilibrium is a valid assumption?**

305 First of all, the validity of the isothermal assumption can be asserted us-  
306 ing numerical simulation. From the numerical results presented in previous  
307 section, the heat power consumed by phase change has been computed along  
308 the soil column for each time step. At short times ( $t < 2$  days), absolute value  
309 of the heat power reaches a maximum of  $4500 \text{ W m}^{-3}$  in the first layer at

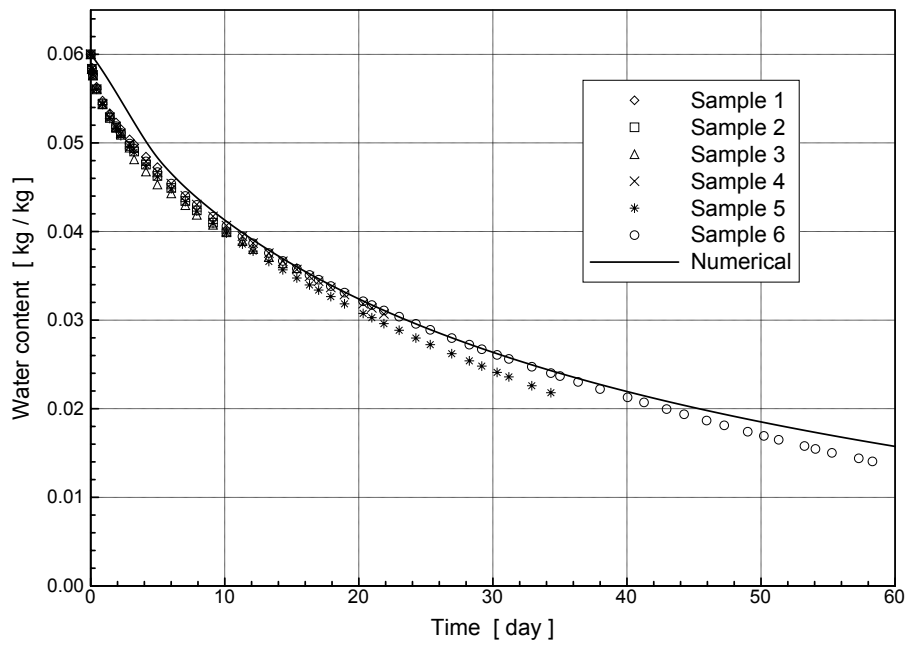


Figure 6: Drying kinetics. Comparison between theoretical prediction and experimental results in the first case:  $RH_1 = 30\%$ .

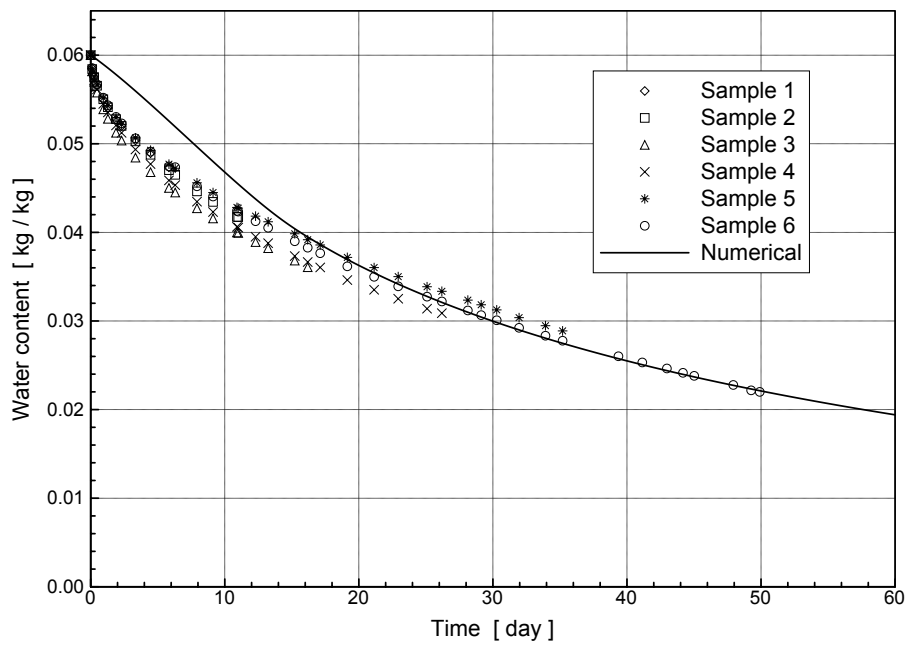


Figure 7: Drying kinetics. Comparison between theoretical prediction and experimental results in the second case:  $RH_2 = 50\%$ .

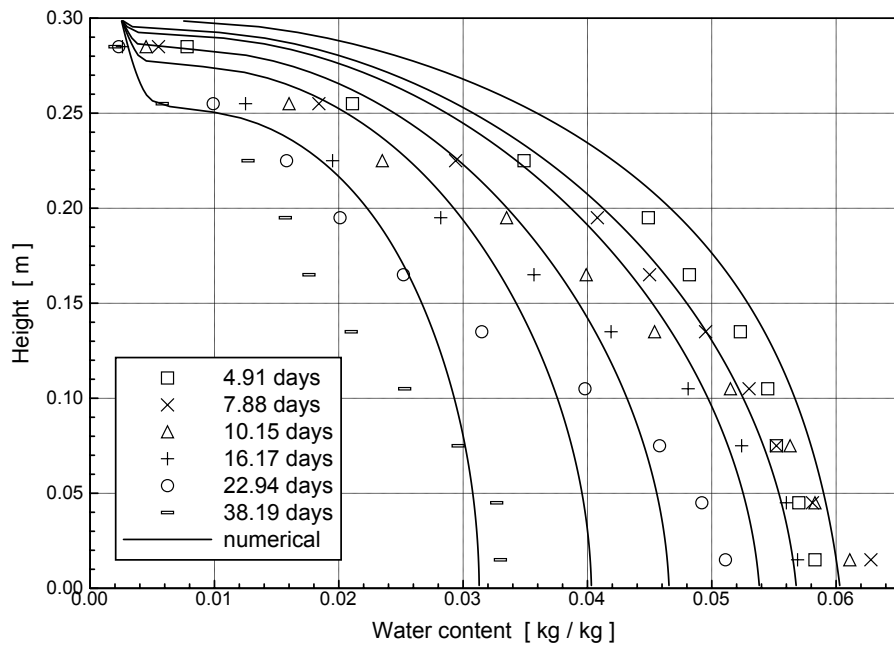


Figure 8: Water content profiles along soil columns. Comparison between theoretical prediction and experimental results in the first case:  $RH_1 = 30\%$ .

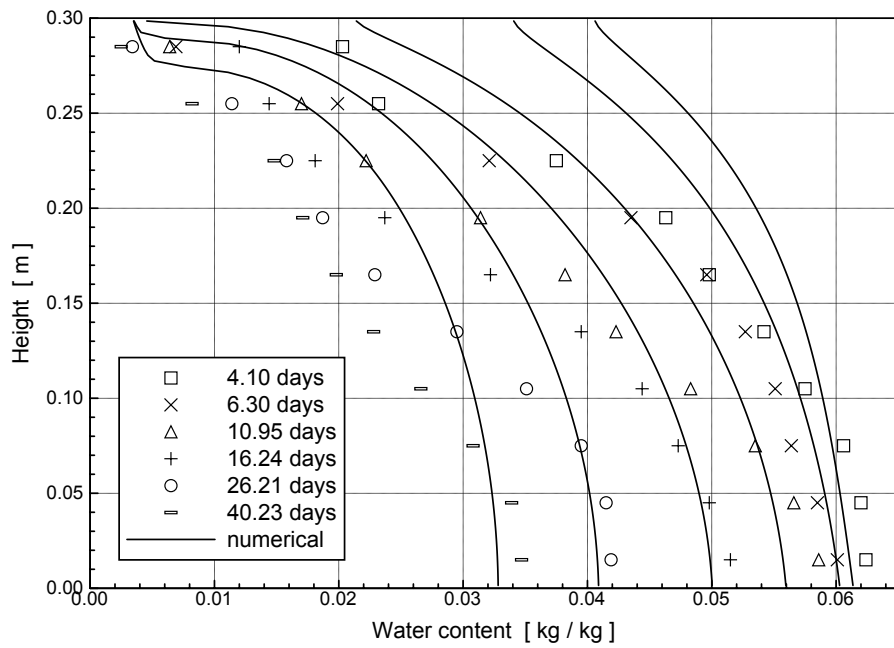


Figure 9: Water content profiles along soil columns. Comparison between theoretical prediction and experimental results in the second case:  $RH_2 = 50\%$ .

310 the upper surface. This value quickly decreases below  $1000 \text{ W m}^{-3}$  reaching  
 311  $80 \text{ W m}^{-3}$  at the end of experiment. Since the heat power is maximal in  
 312 the first layer of soil in contact with the thermo-regulated atmosphere, small  
 313 temperature deviations could be observed in the upper part of soil columns  
 314 in the first 2 days. Temperature gradient would enhance superficial vapour  
 315 flux and eventually speed up the drying process. This issue could account for  
 316 the discrepancies observed in drying kinetics at the beginning of experiments  
 317 (Figs. 6 and 7). Anyway, the heat power computed beyond the first 2 days  
 318 is not sufficient to generate significant temperature deviations. Indeed, the  
 319 isothermal assumption is valid as long as the overall drying kinetics is suffi-  
 320 ciently slow what is fairly verified in the cases under investigation. Further  
 321 work is required to couple our model with heat flows and provide a detailed  
 322 analysis of the isothermal assumption. However, this issue is beyond the  
 323 scope of this paper.

324 Most of water (vapour and liquid) transport models developed to describe  
 325 drying or water management processes relies on the *local equilibrium assump-*  
 326 *tion*. This hypothesis specifies that, on each point of the domain, liquid and  
 327 gas phases are in equilibrium. In our case, it can be written as:

$$\forall t, p_v = p_{veq} \quad (20)$$

328 postulating that the vapour pressure remains at its equilibrium value. Phys-  
 329 ically, it amounts to saying that, when compared to diffusion, phase change  
 330 processes are sufficiently fast to assume it instantaneous. This usual as-  
 331 sumption has been taken into account without carefully checking its domain  
 332 of validity. A large set of experimental investigations on phase change kinet-  
 333 ics have suggested that evaporation in soils may not be as fast as supposed

334 (Bénet and Jouanna, 1982; Lozano et al., 2008; Ruiz and Bénet, 2001). For  
 335 instance, phase change kinetics is drastically decreased when the binding en-  
 336 ergy of water layers adsorbed on fine-scale grains increased (Lozano et al.,  
 337 2009). This is mainly the case in the hygroscopic range of water content and  
 338 is emphasized in the presence of a clayey fraction.

339 To evaluate the liquid/gas non-equilibrium, the ratio of the vapour pres-  
 340 sure divided by its equilibrium value is proposed.

$$\theta = \frac{P_v}{P_{veq}} \quad (21)$$

341 This criterion is plotted along the soil column in Fig. 10. One can note that  
 342 the vapour pressure can strongly deviate from its equilibrium value. Along  
 343 the profile, average and largest value of non-equilibrium are given as functions  
 344 of time in Fig. 11. The short time behaviour ( $t < 4$  days) corresponds to the  
 345 establishment of the vapour profile governed by diffusion. It is a transient  
 346 behaviour which is not of particular interest with regards to the practical  
 347 applications concerned. For larger time ( $t > 10$  days), as transport processes  
 348 are fully established, average non-equilibrium is close to 1 while local values  
 349 can go up to 0.6.

350 Thus, deviation from equilibrium is significant only in a limited region  
 351 ( $0.25 < z < 0.20$ ). To analyse this point, computed water fluxes in liquid  
 352 and gas phases are shown in Fig. 12. Liquid and gas water fluxes are the 1D  
 353 representations of, respectively,  $\rho_l \mathbf{v}_l$  in Eq. 1 and  $\mathbf{J}_v$  in Eq. 2. To compare  
 354 these fluxes with phase change rate, it has been rewritten in terms of surface  
 355 flux:

$$\hat{J}_v = \hat{\rho}_v dz \quad (22)$$

356 where  $dz$  is the spatial discretization used in numerical simulation. The  
357 intensities of water fluxes and phase change rate cannot be directly compared  
358 since they do not take part identically in mass balance equations (Eqs. 11  
359 and 12). Indeed, water fluxes are cumulative through the gradient operator  
360 while phase change is a volumetric rate. Nevertheless, the comparison of the  
361 three plots supports a qualitative analyse.

362 Water flux occurs predominantly in liquid phase in the lower part of  
363 columns and almost exclusively in gas phase in the upper part (Gowing  
364 et al., 2006; Yamanaka and Yonetani, 1999; Yanful and Mousavi, 2003). The  
365 switch from one behaviour to the other occurs precisely in the region where  
366 non-equilibrium is maximum ( $0.25 < z < 0.20$  in Fig. 10). Since the non-  
367 equilibrium criterion corresponds to the generalized thermodynamic force  
368 governing the phase change flux (Eq. 9), phase change rate is maximum in  
369 this region which creates the main source term in vapour transfer processes.  
370 Thus, the 3 water transport phenomena coexist only in this transition zone.

371 As the evaporation front evocated in previous section penetrates in the  
372 soil column, this transition zone propagates from the upper boundary condi-  
373 tion towards soil bottom. This defines the dry surface layer (DSL) a few cen-  
374 timetres below the surface identified by Yamanaka et al. (1998); Yamanaka  
375 and Yonetani (1999). After all, the only manifestation of coupling effects  
376 between liquid and vapour transport mechanisms occurs in a limited region  
377 as well as the deviation from equilibrium. However, this particular zone  
378 governs the overall water transport kinetics. Actually, the cases under inves-  
379 tigation underline that the vapour diffusion is not impeded and that there is  
380 no specific limiting phenomena. Indeed, the kinetics results from a complex

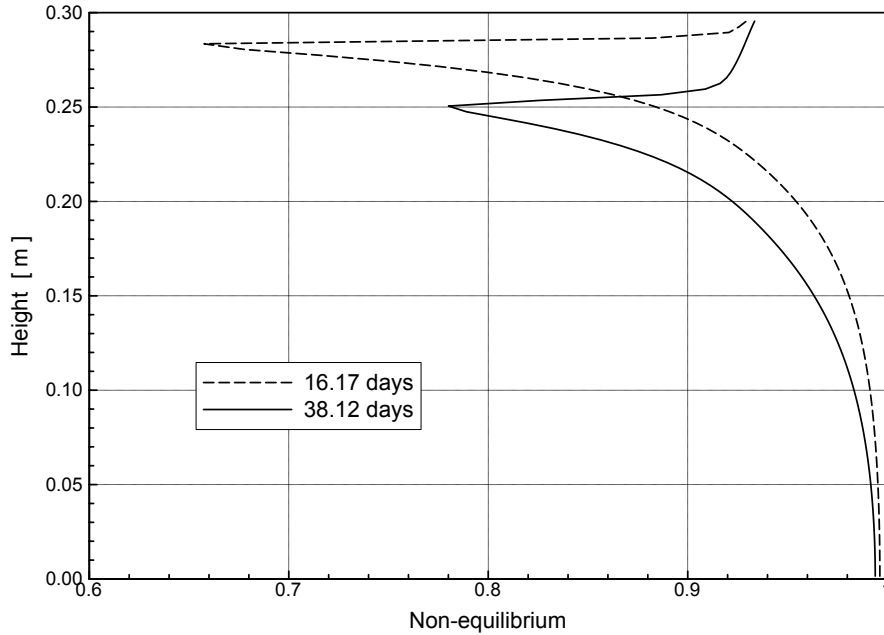


Figure 10: Theoretical liquid/gas non-equilibrium,  $\theta = \frac{p_v}{p_{veq}}$ , along the soil column in the first case:  $RH_1 = 30\%$  at  $t = 38.2$  days.

381 competition of filtration, diffusion and phase change.

382 Taking into account the liquid/gas equilibrium assumption would lead to  
 383 artificially increase the phase change rate and enhance the vapour flux. In  
 384 such a case, the diffusion process would govern the overall kinetics. Since the  
 385 equilibrium vapour pressure is directly linked to the water content through  
 386 the sorption isotherm, the vapour diffusive flux would only depend on the  
 387 water content vertical gradient. This means that a vapour diffusive flux could  
 388 only occur in the hygroscopic domain where equilibrium vapour pressure  
 389 deviates from the saturated vapour pressure. From our mind, this constraint  
 390 is too restrictive while it is usually hidden by the non-isothermal vapour flux.

391 The material used in this work is a fine sand that does not present im-

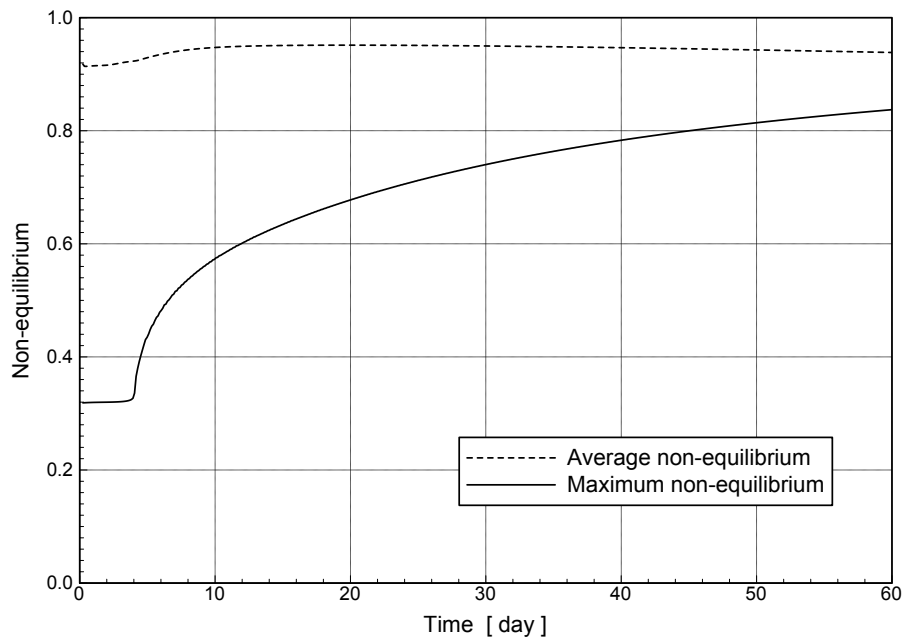


Figure 11: Evolution of maximum and average liquid/gas non-equilibrium,  $\theta = \frac{p_v}{p_{veq}}$ , as function of time in the first case:  $RH_1 = 30\%$ .

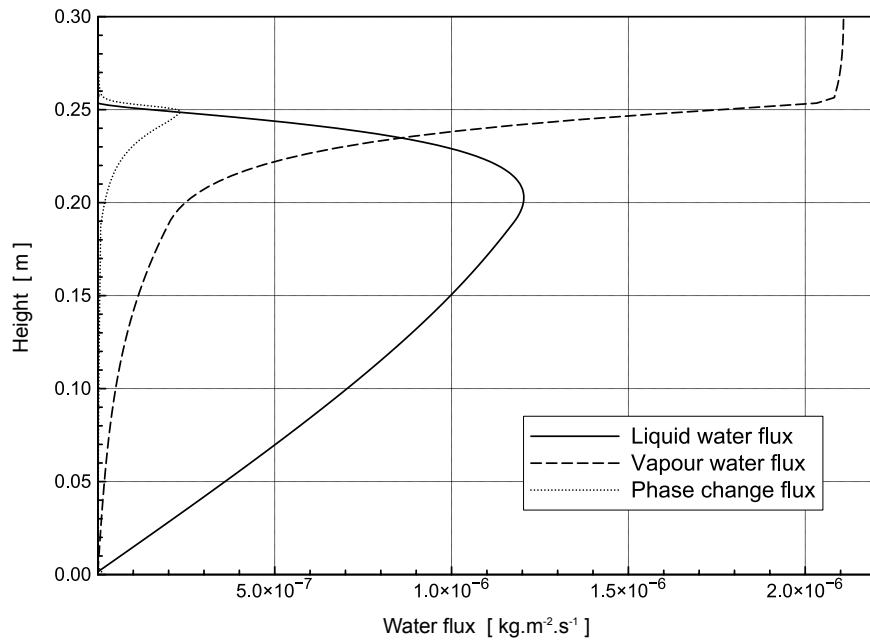


Figure 12: Theoretical water fluxes in gas phase,  $\mathbf{J}_v$ , and liquid phase,  $\rho_l \mathbf{v}_l$ , along the soil column in the first case:  $RH_1 = 30\%$  at  $t = 38.2$  days. The surface representation of phase change rate,  $\hat{J}_v$  (Eq. 22), is added for comparison.

392 portant hygroscopic effects, i.e., the hygroscopic domain represents a limited  
393 range of water content  $0\% < w < 2\%$  (Fig. 2). It has been shown that  
394 phase change rate is drastically lowered as the water activity deviates from  
395 1 (Bénet et al., 2009). For instance, a small clay fraction ( $\approx 10\%$ ) sig-  
396 nificantly increases hygroscopic effects and decreases phase change kinetics  
397 (Lozano et al., 2008). Thus, similar investigations carried out with silty sand  
398 or clayey sand would enhance the liquid/gas non-equilibrium calling for a  
399 two-equation model such as the one developed in this paper.

## 400 **6. Conclusion**

401 By rejecting the local liquid/gas equilibrium assumption, a non-equilibrium  
402 model of isothermal water transport in soil has been proposed. Liquid water  
403 and vapour transport are ruled by 2 mass balance equations while the cou-  
404 pling between them is described by a non-equilibrium phase change relation.  
405 It amounts to consider that the characteristic times associated with each wa-  
406 ter transport mechanism (liquid filtration, vapour diffusion, phase change)  
407 are of the same order of magnitude. By comparing numerical simulations  
408 to drying kinetics and water content profiles obtained from laboratory soil  
409 column experiments, a validation of this description is proposed. It must be  
410 recalled that the comparison test does not rely on any adjusted parameters  
411 since each soil characteristics has been identified with an independent and  
412 specific experimental procedure.

413 In the cases under investigation, local liquid/gas equilibrium can clearly  
414 not be a reasonable assumption. Even if average non-equilibrium is not  
415 particularly pronounced, it is locally significant as the vapour pressure can

416 drop down to half of its equilibrium value. The limited region where a large  
417 non-equilibrium is observed defines the evaporation front. It corresponds to  
418 the transition from liquid transport in deeper layers to vapour transport in  
419 superficial layers which controls the moisture dynamics in bare soils. From  
420 this model, the overall evaporation rate can be estimated directly without  
421 resorting to empirical correlations (Bittelli et al., 2008; Yanful and Mousavi,  
422 2003).

423 The more questionable aspect of this model concerns the description of  
424 the relative permeability function. Indeed, it is now well established that the  
425 relation proposed by Van Genuchten (1980) is not appropriate at low water  
426 content. Further investigations are required to develop accurate modelling of  
427 liquid flow phenomena at very low water content as proposed by Tuller and  
428 Or (2002) and Peters and Durner (2002).

429 Since the coupling with heat flux is not taken into account, this model  
430 cannot be applied directly on practical situations to describe natural field  
431 observations. It is rather an heuristic model dedicated to discuss the local  
432 equilibrium assumption and assess its eventual reliability. Atmospheric ther-  
433 mal evolutions highly influence water content dynamics in the first layers of  
434 bare soils, particularly in arid regions where diurnal temperature variations  
435 are large (Gowing et al., 2006). Thus, the approach proposed in this work  
436 must be included in a wider modelling such as existing land-surface models  
437 (Garcia-Gonzalez et al., 2012; Simunek et al., 2008).

438 As evidenced previously, phase change kinetics is highly influenced by  
439 hygroscopic effects (Lozano et al., 2008). For instance, a clayey fraction will  
440 decrease the phase change rate and extend the hygroscopic domain. Such a

441 situation would lead to intensify non-equilibrium, or at least to widen the  
442 transition zone and the evaporation front. In this framework, the introduc-  
443 tion of organic matter like compost should modify the moisture dynamics.  
444 Based on this approach, our objective is to revisit the traditional techniques  
445 developed in subsaharian regions to prevent from soil evaporation and opti-  
446 mize water resources management.

## 447 **References**

448 Abu-El-Shar, W.Y., Abriola., L.M., 1997. Experimental Assessment of Gas  
449 Transport Mechanisms in Natural Porous Media: Parameter Evaluation.  
450 Water Resources Research 33, 505–516.

451 Armstrong, J., Frind, E., McClellan, R., 1994. Non-equilibrium mass transfer  
452 between the vapor, aqueous, and solid phases in unsaturated soils during  
453 vapor extraction. Water Resources Research 30, 355–368.

454 Baker, R. and Frydman, S., 2009. Unsaturated soil mechanics critical review  
455 of physical foundations. Engineering Geology 106, 26–33.

456 Bedeaux, D., Kjelstrup, S., 2004. Irreversible thermodynamics - A tool to de-  
457 scribe phase transitions far from global equilibrium. Chemical Engineering  
458 Science 59, 109–118.

459 Bénet, J.C., Jouanna, P., 1982. Phenomenological relation of phase change of  
460 water in a porous medium: experimental verification and measurement of  
461 the phenomenological coefficient. International Journal of Heat and Mass  
462 Transfer 25, 1747–1754.

- 463 Bénéet, J.-C., Lozano, A.-L., Cherblanc, F., Cousin, B., 2009. Phase change  
464 of water in hygroscopic porous medium. phenomenological relation and  
465 experimental analysis for water in soil. *Journal of Non Equilibrium Ther-*  
466 *modynodynamics* 34, 133–153.
- 467 Bénéet, J.-C., Ramirez-Martinez, A., Ouedraogo, F., Cherblanc, F., 2012.  
468 Measurement of the chemical potential of a liquid in porous media. *Journal*  
469 *of Porous Media* 15, 1019–1029.
- 470 Bittelli, M., Ventura, F., Campbell, G.S., Snyder, R.L., Gallegati, F., Pisa,  
471 P.R., 2008. Coupling of heat, water vapor, and liquid water fluxes to com-  
472 pute evaporation in bare soils. *Journal of Hydrology* 362, 191–205.
- 473 Campbell, G. S., 1985. *Soil physics with BASIC*, Elsevier, New-York.
- 474 Chammari, A., Naon, B., Cherblanc, F., Cousin, B., Bénéet, J.C., 2008. Inter-  
475 preting the drying kinetics of a soil using a macroscopic thermodynamic  
476 non-equilibrium of water between the liquid and vapour phase. *Drying*  
477 *Technology* 26, 836–843.
- 478 Fredlund, D.G., Xing, A., 1994. Equation for the Soil-Water Characteristic  
479 Curve. *Canadian Geotechnical Journal* 31, 521–532.
- 480 Fredlund, M.D., Wilson, G.W., Fredlund, D.G., 2002. Use of the grain-size  
481 distribution for estimation of the soil-water characteristic curve. *Canadian*  
482 *Geotechnical Journal* 39, 1103–1117.
- 483 Garcia-Gonzalez, R., Verhoef, A., Vidale, P.L. and Braud, I., 2012. Incorporation  
484 of water transport in the JULES land surface model: Implications

- 485 for key soil variables and land surface fluxes. *Water Resources Research*  
486 48, W05538.
- 487 Grifoll, J., Gasto, J.M., Cohen, Y., 2005. Non-isothermal soil water transport  
488 and evaporation. *Advances in Water Resources* 28, 1254–1266.
- 489 Gowing, J.W., Konukcu, F., Rose, D.A., 2006. Evaporative flux from a shal-  
490 low watertable: The influence of a vapour-liquid phase transition. *Journal*  
491 *of Hydrology* 321, 77–89.
- 492 Job, G., Hermann, F., 2006. Chemical potential, a quantity in search of  
493 recognition. *European Journal of Physics* 27, 353–371.
- 494 Kuiken, G.D.C., 1994. *Thermodynamics for Irreversible Processes*. Wiley,  
495 Chichester.
- 496 Lozano, A.-L., Cherblanc, F., Cousin, B. and Bénét, J.-C., 2008. Experi-  
497 mental study and modelling of the water phase change kinetics in soils.  
498 *European Journal of Soil Science* 59, 939–949.
- 499 Lozano, A.-L., Cherblanc, F., Bénét, J.-C., 2009. Water evaporation versus  
500 condensation in a hygroscopic soil. *Transport in Porous Media* 80, 209–222.
- 501 Low, P. F., 1961. Concept of total potential in water and its limitations: A  
502 critique. *Soil Science* 91, 303–305.
- 503 Moldrup, P., Olesen, T., Gamst, J., Schjønning, P., Yamaguchi, T., Rolston,  
504 D. E., 2000. Predicting the gas diffusion coefficient in repacked soil: Water-  
505 induced linear reduction model. *Soil Sci. Soc. Am. J.* 64, 1588–1594.

- 506 Moldrup, P., Olesen, T., Komatsu, T., Schjønning, P. and Rolston, D. E.,  
507 2001. Tortuosity, diffusivity, and permeability in the soil liquid and gaseous  
508 phases. *Soil Sci. Soc. Am. J.* 65, 613–623.
- 509 Nitao, J.J., Bear, J., 1996. Potentials and their role in transport in porous  
510 media. *Water Resources Research* 32, 225–250.
- 511 Novak, M.D., 2010. Dynamics of the near-surface evaporation zone and cor-  
512 responding effects on the surface energy balance of a drying bare soil.  
513 *Agricultural and Forest Meteorology* 150, 135–1365.
- 514 Parlange, M. B., Cahill, A. T., Nielsen, D. R., Hopmans, J. W., Wendroth,  
515 O., 1998. Review of heat and water movement in field soils. *Soil & Tillage*  
516 *Research* 47, 5–10.
- 517 Peters, A., Durner, W., 2008. A simple model for describing hydraulic con-  
518 ductivity in unsaturated porous media accounting for film and capillary  
519 flow. *Water Resources Research* 44: W11417, doi:10.1029/2008WR007136.
- 520 Rose, D.A., Konukcu, F., Gowing, J.W., 2005. Effect of watertable depth  
521 on evaporation and salt accumulation from saline groundwater. *Australian*  
522 *Journal of Soil Research* 43, 565–573.
- 523 Ruiz, T., Bénet, J.-C., 2001. Phase change in a heterogeneous medium: com-  
524 parison between the vaporization of water and heptane in an unsaturated  
525 soil at two temperatures. *Transport in Porous Media* 44, 337–353.
- 526 Saito, H., Simunek, J., Mohanty, B.P., 2006. Numerical analysis of coupled  
527 water, vapor and heat transport in the vadose zone. *Vadose Zone Journal*  
528 5, 784–800.

- 529 Sakai, M., Toride, N., Simunek, J., 2009. Water and Vapor Movement with  
530 Condensation and Evaporation in a Sandy Column. *Soil Science Society  
531 of America Journal* 73, 707–717.
- 532 Simunek, J., van Genuchten, M.T., Sejna, M., 2008. Development and ap-  
533 plications of the HYDRUS and STANMOD software packages and related  
534 codes. *Vadose Zone Journal* 7, 587–600.
- 535 Thakur, V.K.S., Sreedeeep, S., Singh, D.N., 2006. Laboratory investigations  
536 on extremely high suction measurements for fine-grained soils. *Geotechni-  
537 cal and Geological Engineering* 24, 565–578.
- 538 Thomas, H.R., Missoum, H., 1999. Three-dimensional coupled heat, moisture  
539 and air transfer in a deformable unsaturated soil. *International Journal for  
540 Numerical Methods in Engineering* 44, 919–943.
- 541 Tuller, M., Or, D., 2002. Unsaturated Hydraulic Conductivity of Structured  
542 Porous Media: A Review of Liquid ConfigurationBased Models. *Vadose  
543 Zone Journal* 1, 14–37.
- 544 Van Genuchten, M.T., 1980. A closed-form equation for predicting the hy-  
545 draulic conductivity of unsaturated soils. *Soil Science Society of America  
546 Journal* 44, 892–898.
- 547 Van Genuchten, M.T., Nielse, D.R., 1985. On describing and predicting the  
548 hydraulic properties of unsaturated soils. *Annales Geophysicae* 3, 615–628.
- 549 Xiang, L., Yu, Z., Chen, L., Mon, J., Lu, H., 2012. Evaluating coupled  
550 water, vapor and heat flows and their influence on moisture dynamics in  
551 arid regions. *Journal of Hydrologic Engineering* 17, 565–577.

- 552 Yamanaka, T., Takeda, A., Shimada, J., 1998. Evaporation beneath the soil  
553 surface: some observational evidences and numerical experiments. Hydro-  
554 logical Processes 12, 21932203.
- 555 Yamanaka, T., Yonetani, T., 1999. Dynamics of the evaporation zone in dry  
556 sandy soils. Journal of Hydrology 217, 135–148.
- 557 Yanful, E.K., Mousavi, S.M., 2003. Estimating falling rate evaporation from  
558 finite soil columns. The Science for the Total Environment 313, 141–152.